RELIABILITY MODELING OF BRITTLE ANISOTROPIC MATERIALS

Jonathan Salem, Ronald Noebe and Jane Manderscheid
NASA Lewis Research Center
Cleveland, OH 44135

INTRODUCTION

Single-crystal NiAl alloys offer numerous property advantages over their Ni-based single-crystal superalloy counterparts for applications in high pressure turbine engine sections [1]. These advantages include higher melting point, greater thermal conductivity, better oxidation resistance, a better response to thermal barrier coatings, and a reduction in density by as much as a third without significantly sacrificing creep strength. The current drawback is their lack of ductility and their anisotropy of both strength and elastic response. The material considered herein exhibits a fracture toughness of 3-5 MPa$\sqrt{m}$ [2], while Young's modulus varies from 96 to 275 GPa and the strength varies by a factor of two depending on orientation. Consequently, a significant effort is being made to develop testing and design methodologies that will account for the lack of ductility and the strength anisotropy exhibited by brittle single crystals such as NiAl.

The present approach is to modify existing test methods and brittle design methodologies, such as those applied to ceramics and glasses [3], and to experimentally verify the results. This paper focuses on the basic materials properties and strength behavior of a NiAl single crystal alloy and the development of a reliability model for the design of components subjected to multiaxial stresses.

EXPERIMENTAL PROCEDURE

Material Preparation

Single crystal billets of a NiAl alloy designated AFN12 were mounted on goiniometers and oriented by X-ray diffraction. Flexural specimens, measuring 3 by 4 by 45 mm in thickness, depth and length, respectively, were then cut from the billets along the <001> or <110> axes by electro-discharge machining (EDM). The resulting surfaces were sanded with 400 grit silicon carbide paper and chemically milled in a solution of phosphoric and nitric acid to remove the EDM damage.

Elastic Properties

Sonic moduli of the flexural specimens were measured by using the impulse excitation technique [4]. Specimens were supported at the nodal points with foam strips and the specimen impacted lightly with an appropriate hammer. The resultant impact induced flexural vibration that was detected with a piezoelectric crystal placed on the specimen and automatically recorded with an electronic circuit. The elastic moduli were then calculated from the specimen geometry and measured resonant frequency.

Uniaxial Flexural Strength Testing

Strength was determined by loading the specimens in three- or four-point flexure at a strain rate of 10^{-4}/min [5] on a support span of 40 mm. The loading span for four-point flexure was 20 mm. A fully articulated flexure fixture, which allowed each loading pin to roll along and rotate about the specimen long axis, was used to accommodate any machining run-outs induced in specimen preparation.

RESULTS

Elastic Properties

The measured elastic moduli were $E_{<001>} = 96.9 \pm 1.0$ GPa and $E_{<110>} = 187 \pm 2.4$ GPa. Both values are in good agreement with the data of Wasilewski [6] for binary NiAl, implying that the single crystal elastic constants for binary NiAl sufficiently represent this material for engineering purposes. However, a minor discrepancy can be noted in Wasilewski's data: The constants given in dynes/cm^2 disagree with those given in pounds/in^2 by a factor of 1.5% [7]. The values given in dynes/cm^2 gave the best agreement and were used herein.

The elastic constants [6] were used to calculate the elastic modulus of NiAl on the (100) and (110) planes, as shown in Figs. 1 and 2. The elastic modulus reaches a minimum of 95.9 GPa in the <100> and a maximum of 275 GPa in the <111> with an intermediate value of 187 GPa in the <110>.

Uniaxial Flexural Strength

The flexural strengths of the material in the <001> and the <110> directions are summarized in Tables I and II. The results imply that the strength is a function of both test specimen orientation and volume.

Fractography, which will be presented below, indicates brittle failure with the failure originating from surface flaws on the test section without bulk deformation. Localized deformation could not be observed about the failure origins if it existed. Thus, failure appears to be of the weakest link type and Weibull statistics [3] should reasonably characterize the results from a phenomenological viewpoint. The probability of failure, F, for such behavior under uniaxial loading is given by

$$F = 1 - EXP\left(-\int_A \left(\frac{\sigma}{\sigma_o}\right)^m dA\right) \qquad \text{or} \qquad F = 1 - EXP\left(-\int_A k_{ws}(\sigma)^m dA\right) \tag{1}$$

where σ is the applied stress, σ_o is the scale parameter and corresponds to a unit area of material stressed in uniform tension, m is the Weibull modulus (or shape parameter) and k_{ws} is the crack density coefficient [8]. The integral is taken over the volume of the specimen if failure occurs from internal defects or over the area, as indicated above, if failure initiates from the surface. If both surface and volume defects induce failure, then both probabilities can be calculated and combined.

The resulting probabilities of failure as a function of stress are shown in Fig. 3 for the <001> and <110> orientations. In order to determine if the differences in characteristic strength and Weibull modulus were statistically significant, 90% confidence bands were determined [9]. As seen in Table I, significant strength differences exist between the three- and four-point configurations for both orientations, and between orientations for the same configuration. However, significant differences

Table I: Weibull strength statistics of single crystal NiAl AFN12

Orientation and Flexural Configuration	Failure@ Location and Type	Characteristic Strength σ_θ, MPa	90% Confidence Bands, σ_θ	Weibull* Modulus m_s	90% Confidence Bands on m_s	Predicted Characteristic Strength
<100> 3-point	S-Carbide	1350	1258 to 1475	6.1	4.4 to 8.5	—
<100> 4-Point	S-Carbide	1094	1032 to 1158	5.4	4.3 to 6.8	1040
<110> 3-Point	S-Carbide	843	754 to 933	4.8	2.2 to 9.2	—
<110> 4-Point	S-Carbide	689	642 to 735	5.5	3.5 to 8.2	653
<110> 3-Point	S-EDM	—	—	—	—	—
<110> 4-Point	S-EDM	474	—	4.6	—	—

Table II: Normal strength statistics for single crystal NiAl AFN12

Orientation and Flexural Configuration	Failure@ Location and Type	Number of Test	Mean# Strength MPa	Standard Deviation of Strength SD_σ, MPa	Coefficient of Variation CV_σ
<100> 3-point	S-Carbide	15	1261	209	0.17
<100> 4-Point	S-Carbide	32	1010	202	0.20
<110> 3-Point	S-Carbide	9	767	177	0.23
<110> 4-Point	S-Carbide	15	629	130	0.21
<110> 3-Point	S-EDM	3	466	69	0.15
<110> 4-Point	S-EDM	19	340	107	0.31

@ S = surface; EDM = electo-discharge machining scar. # Mean strength with one standard deviation.
* Weibull modulus and characteristic strength were determined with the maximum likelihood method.

could not be detected between the Weibull moduli for the three- and four-point configurations for either orientation, or between orientations for the same configuration

Metallographic studies [10] of the flaw distribution of this alloy indicate no strong bias with orientation, Thus, the difference in strength between the <001> and the <110> orientations appears to result from the difference in fracture toughness with orientation [2] instead of a difference in flaw distribution.

Fractography

The fracture surface of the specimens were observed with a scanning electron microscope and analyzed with energy and wavelength dispersive spectrometers. The <001> specimens failed from coarse metal-carbide particles as summarized in Table II. However, over one-half of the <110> specimens failed from machining damage, even though all the specimens were prepared together by the same method. This reflects the low fracture toughness of NiAl on the (110) plane [2] and possibly a difference in the chemical milling with orientation. Typical examples of carbide and machining failures are shown in Figs. 4 and 5.

EFFECT OF TEST SPECIMEN VOLUME

If Equation (1) is equated to itself for two different specimen configurations, the following scaling equation can be derived for a given probability of failure:

$$\sigma_1/\sigma_2 = \left(A_{e2}/A_{e1}\right)^{1/m} \tag{2}$$

where σ_i is the strength corresponding to effective area A_{ei}. As the specimens in this study failed from surface connected flaws, use of an effective area is appropriate. The effective area for three- or four-point flexure is

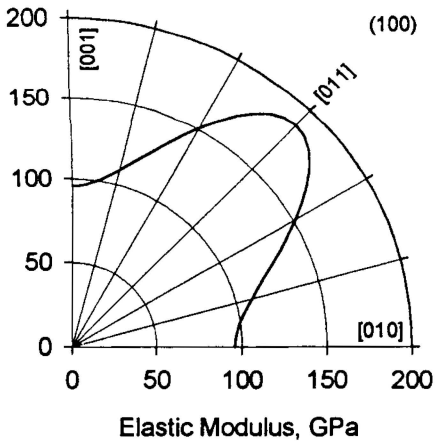


Fig. 1: The elastic modulus $E_{[hkl]}$ of binary NiAl as a function of orientation on the (100).

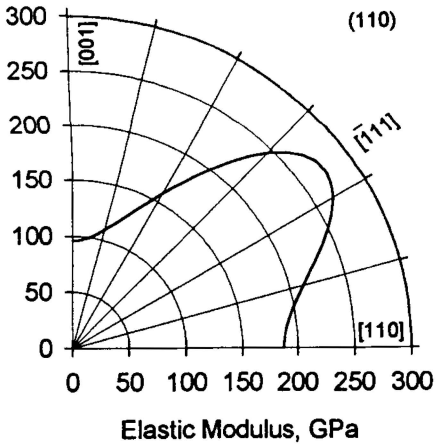


Fig. 2: The elastic modulus $E_{[hkl]}$ of binary NiAl as a function of orientation on the (110).

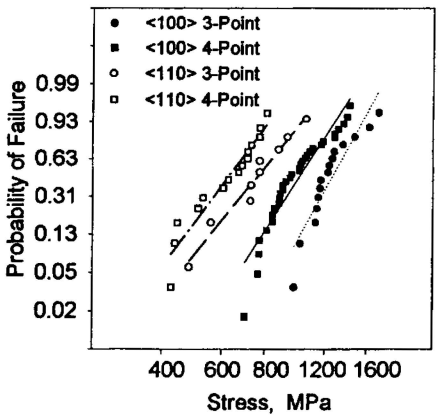


Fig. 3: Weibull flexural strength distributions for <100> and <110> orientations of NiAl.

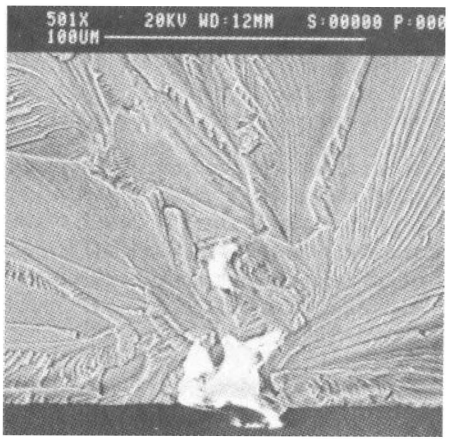


Fig. 4: Failure origin in a <001>flexure specimen. Failure occurred from a metal-carbide particle.

$$A_e = \left[\frac{1+m_s\left(s_i/s_o\right)}{\left(m_s+1\right)^2}\right]\left[1+\frac{m_s w}{w+h}\right][w+h]s_o \tag{3}$$

where m_s is the Weibull modulus for the surface flaw population, s_o and s_i are the outer (support) and inner (loading) spans, respectively, and h and w are the height and depth of the beam, respectively [11]. Equations 3 and 4 are generally considered capable of predicting four-point strengths from three-point strength data for brittle, isotropic materials such as ceramics and glasses. To determine the applicability of these scaling equations to this single crystal NiAl alloy, the average of the Weibull moduli in Table I was used to calculate the effective areas and predict the four-point strength from the three-point data. The predictions agree well with the experimental results, as shown in Table I. Thus, the probability of failure for uniaxial flexure of this single crystal can be described by

$$F = 1 - EXP\left(-\int_A\left(\frac{\sigma_{n<hkl>}}{\sigma_{o<hkl>}}\right)^m dA\right) \quad \text{or} \quad F = 1 - EXP\left(-\int_A k_{ws}\left(\sigma_{n<hkl>}\right)^m dA\right) \tag{4}$$

where the subscript *<hkl>* specifies the crystal direction normal to the *(hkl)* plane and k_{ws} is a crack density coefficient dependent on the orientation of the applied stress:

$$k_{ws} = \left(\sigma_{o<hkl>}\right)^{-m} \tag{5}$$

Note that this material does exhibit yield in compression at approximately 1650 MPa in the <001> and at 1050 MPa in the <110> [12]. It is unknown if this phenomenon is volume dependent, however, deformation is typically not viewed as volume dependent. Thus, for a sufficiently small test volume, yield, rather than brittle fracture, might occur. Equations (2) and (3) indicate that a miniature, <001> three-point flexure specimen with 1 by 1.5 mm cross section and a 6 mm support span would have a 10% chance of failing at a tensile stress equal to the compressive yield stress. As yield in compression and tension generally require the same absolute stress, the implication is that very localized (e.g. contact) stresses, such as those at the root of a blade or vane, might be overcome by yield rather than brittle fracture.

MULTIAXIAL RELIABILITY MODELS

One simple model used to predict the reliability of components made from brittle, isotropic materials is the principal of independent action (PIA) model[13]

$$F = 1 - EXP\left\{-\int_A\left[\left[\frac{\sigma_1}{\sigma_o}\right]^m + \left[\frac{\sigma_2}{\sigma_o}\right]^m dA\right\}\right. \tag{6}$$

where the σ_i *'s (i = 1,2)* are the principal stress components greater than zero, σ_o is the scale parameter and m the Weibull modulus. For brittle materials, such as glasses and ceramics, the compressive strength is substantially larger than the tensile strength and compressive stresses are ignored in many applications. However, as noted above, this NiAl alloy exhibits strength anisotropy and will yield in compression. Thus the principal stresses may not be oriented on the weakest planes or they may be oriented on those that will yield in compression. Further, as seen in Fig. 4, the flaws are complex three dimensional objects that may transmit tractions across the interface, instead of planar cracks with a random orientation.

Thus the PIA model needs modification to consider the effects of normal stresses on a multiplicity of planes with various effective strengths, or at least the most significant planes and the corresponding effective strengths, leading to

$$F = 1 - EXP\left(-\int_A \left[\sum \left(\frac{\sigma_{n<hkl>}}{\sigma_{o<hkl>}} \right)^m \right] dA \right) \tag{7}$$

where the summation is taken over the most significant planes (i.e. the weak cleavage planes and those subjected to all the principals). Two extreme cases of Eq. (7) can be considered: That in which a single term in the series dominates reliability and that in which all normal stresses reduce reliability. The first case occurs if a strong maximum in the stress distribution exists and is oriented on or near a weak cleavage plane; the term in the summation is the ratio of the maximum normal stress to minimum characteristic strength. The second case is the limit in which the summation term becomes an integral over all crystal directions. This would appear very conservative, even though the normal stress component in any direction should reduce the reliability associated with flaws like those shown in Figs. 4 and 5. Such an effect was proposed by Weibull [3] via the normal stress averaging technique which is written as

$$F = 1 - EXP\left(-\int_A k_{wps} (\bar{\sigma}_n)^m \right) dA \tag{8}$$

where the averaged normal stress about a unit circle is

$$\bar{\sigma}^m_n = \int_C \sigma^m_n dC \Big/ \int_C dC \tag{9}$$

As the scale parameter is a function of orientation for an anisotropic material, Eq. (8) can be generalized to

$$F = 1 - EXP\left\{ -\int_A \left[\bar{N}^m_n \right] dA \right\} \tag{10}$$

where the averaged normal stress to strength ratio about a unit circle is

$$\bar{N}^m_n = \int_C \left(\frac{\sigma_{n<hkl>}}{\sigma_{o<hkl>}} \right)^m dC \Big/ \int_C dC \,. \tag{11}$$

Eqs. (10) and (11) can be generalized further by replacing the normal stress with a mode I equivalent stress derived from any appropriate fracture mechanics failure criterion, leading to

$$F = 1 - EXP\left(-\int_A \frac{1}{\pi} \int_0^{\pi} \left(\frac{\sigma_{1eq<hkl>}}{\sigma_{o<hkl>}} \right)^m dC\, dA \right) \tag{12}$$

where and $\sigma_{1eq<hkl>}$ is the mode one equivalent stress parallel to the *<hkl>* direction and normal to the *(hkl)* plane at a location.

For a single free surface stressed in tension the contour integral is taken over all *<hkl>* directions on the *(mno)* plane. If the (100) plane is considered, the scale parameter repeats every quadrant due to crystal symmetry and can be described by

$$\sigma_{o(100)<hkl>} = \sigma_{o[001]} \cos^2(2\theta) + \sigma_{o[011]} \cos^2\left(2\theta + \frac{\pi}{2} \right) \tag{13}$$

where θ is the angle from the [100]. The strength envelope as measured experimentally (i.e. the characteristic strength) can be described with the same functional form, as shown in Fig. 6 for this NiAl alloy.

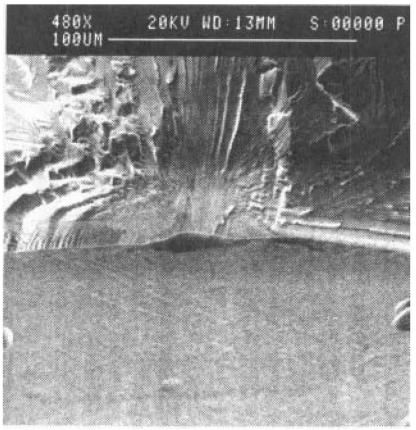


Fig. 5: Failure origin in a <110> flexure specimen. Failure occurred from an EDM scar.

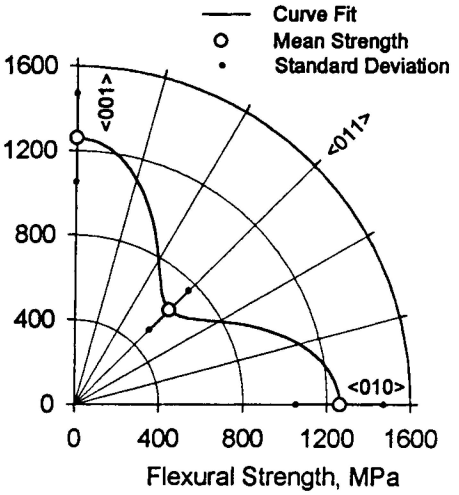


Fig. 6: Characteristic strength of the single crystal NiAl alloy as a function of orientation.

FAILURE CRITERION

The coplanar energy release rate can be used to derive a mode I equivalent stress failure criterion for an anisotropic material. The mode I equivalent energy release rate can be defined as [14]

$$G_{Ieq} = G_I + G_{II} \tag{14}$$

with

$$G_I = -\frac{K_I^2}{2\pi} a_{22} \mathrm{Im}\left\{\frac{\mu_1 + \mu_2}{\mu_1 \mu_2}\right\} \quad \text{and} \quad G_{II} = \frac{K_{II}^2}{2\pi} a_{11} \mathrm{Im}\{\mu_1 + \mu_2\} \tag{15}$$

where the a_{ii}'s are the single crystal elastic constants (compliances), K_I and K_{II} are the mode I and II stress intensity factors defined as $K_I = \sigma_n \sqrt{\pi a}$ and $K_{II} = \tau \sqrt{\pi a}$ where a is the crack size, σ_n is the normal stress and τ is the shear stress. The quantities μ_1 and μ_2 are the roots of the complex equation[15]

$$a_{11}\mu^4 - 2a_{16}\mu^3 + (2a_{12} + a_{66})\mu^2 - 2a_{26}\mu + a_{22} = 0 \ . \tag{16}$$

The equivalent stress can be found by defining the mode I equivalent stress intensity as

$$K_{Ieq} = \sigma_{Ieq} \sqrt{\pi a} \tag{17}$$

and substituting Eqs. (15) and (17) into (14), leading to

$$\sigma_{Ieq} = \sqrt{\sigma_n^2 - \tau^2 \frac{a_{11}}{a_{22}} \frac{\mathrm{Im}(\mu_1 + \mu_2)}{\mathrm{Im}\left[(\mu_1 + \mu_2)/(\mu_1 \mu_2)\right]}} \ . \tag{18}$$

Eqs. (12), (13) and (18) define the necessary functions for reliability analysis of anisotropic, brittle materials. For a volume analysis, more general equations are required.

CONCLUSIONS

As in other brittle materials, an effect of stressed volume exists for this single crystal NiAl alloy. The Weibull scaling law appears to apply to uniaxial cases for effective surface area changes of 300% or less. No statistically significant difference between <110> and <100> Weibull moduli could be detected at 90% confidence. The same flaw population and failure mechanism (brittle failure without macroscopic ductility) appears to control failure in both orientations tested. Strength in the <110> is approximately two thirds of that in the <001>. The strength varies with orientation because fracture toughness varies with orientation. A Weibull-based reliability model and failure criterion for application to brittle materials with strength and elastic anisotropy was derived. The model should also be applicable to isotropic materials that have strength anisotropy due to a nonuniform flaw distribution.

ACKNOWLEDGMENT: The authors thank the Department of Energy Office of Transportation Technologies for funding the research under contract 880R21749.

REFERENCES

1. R. Darolia, "NiAl For Turbine Airfoil Applications," in *Structural Intermetallics*, ed. R. Darolia et al., TMS Warrendale, PA, pp. 495-504, 1993.
2. K. Chang, R. Darolia and H. Lipsitt, "Cleavage Fracture in B2 Aluminides," *Acta Metall.* Vol. 40, No. 10, 1992, pp. 2727-2737.
3. W. Weibull, "A Statistical Theory of the Strength of Materials," *Ingeniors Vetenskaps Akademien Handlinger*, No. 151, 1939.
4. ASTM C 1259-94 "Standard Test Method for Dynamic Young's Modulus, Shear Modulus, and Poisson's Ratio for Advanced Ceramics by Impulse Excitation of Vibration," American Society for Testing and Materials Annual Book of Standards, Vol. 15.01, pp. 336-384, 1995.
5. ASTM C 1161-90 "Standard Test Method for Flexural Strength of Advanced Ceramics at Ambient Temperature," *ibid*, Vol. 15.01, pp. 333-339, 1990.
6. R.J. Wasilewski, "Elastic Constants and Young's Modulus of NiAl", *Transactions of the Metallurgical Society of AIME*, Vol. 236, pp. 455-456, 1966.
7. E.A. Mechtly, "Physical Constants and Conversion Factors," NASA SP-7012, 1973.
8. S.B. Batdorf, "Fundamentals of the Statistical Theory of Fracture," in *Fracture Mechanics of Ceramics*, Vol. 3, ed. R. C. Bradt, et al., Plenumn Press, NY, pp. 1-30, 1978.
9. R.B. Abernethy, J.E. Breneman, C.H. Medlin, G.L. Reinman, G. L., *"Weibull Analysis Handbook,"* AFWAL-TR-83-2079, 1983.
10. R.D. Noebe, P.O. Dickerson, A. Garg, "Hierarchical Characterization of the Microstructure of Single Crystal NiAl Alloy AFN12," NASA TM 107029, 1995.
11. N. Nemeth, J. Manderscheid, J. Gyekenyesi, "CARES Users and Programmers Manual," NASA Technical Paper TP2916, 1990.
12. R.D. Noebe, and A. Garg, "Deformation Behavior of Single Crystal NiAl Alloy D176, NASA Technical Memorandum 106891, 1995.
13. R.L. Barnett, et al., "Fracture of Brittle Materials Under Transient Mechanical and Thermal Loading," U. S. Air Force Flight Dynamics Laboratory. AFFDL-TR-66-220, March, 1967.
14. P.C. Paris and G.C. Sih "Stress Analysis of Cracks," *Fracture Toughness Testing and Its Applications*, American Society for Testing and Materials, STP 381, 1965.
15. S.G. Lekhnitskii, *"Theory of Elasticity of an Anisotropic Body,"* Holden-Day, San Francisco, 1963.